Abnormal phagocytosis by retinal pigmented epithelium that lacks myosin VIIa, the Usher syndrome 1B protein

Daniel Gibbs*, Junko Kitamoto*, and David S. Williams†

Departments of Pharmacology and Neurosciences, School of Medicine, University of California at San Diego, La Jolla, CA 92093-0912

Edited by Jeremy Nathans, The Johns Hopkins University School of Medicine, Baltimore, MD, and approved April 8, 2003 (received for review January 24, 2003)

Mutations in the myosin VIIa gene (*MYO7A*) cause Usher syndrome type 1B (USH1B), a major type of the deaf-blind disorder, Usher syndrome. We have studied mutant phenotypes in the retinas of *Myo7a* mutant mice (shaker1), with the aim of elucidating the role(s) of myosin VIIa in the retina and what might underlie photoreceptor degeneration in USH1B patients. A photoreceptor defect has been described. Here, we report that the phagocytosis of photoreceptor outer segment disks by the retinal pigment epithelium (RPE) is abnormal in *Myo7a* null mice. Both *in vivo* and in primary cultures of RPE cells, the transport of ingested disks out of the apical region is inhibited in the absence of Myo7a. The results with the cultured RPE cells were the same, irrespective of whether the disks came from wild-type or mutant mice, thus demonstrating that the RPE is the source of this defect. The inhibited transport seems to delay phagosome–lysosomal fusion, as the degradation of ingested disks was slower in mutant RPE. Moreover, fewer packets of disk membranes were ingested *in vivo*, possibly because retarded removal of phagosomes from the apical processes inhibited the ingestion of additional disk membranes. We conclude that Myo7a is required for the normal processing of ingested disk membranes in the RPE, primarily in the basal transport of phagosomes into the cell body where they then fuse with lysosomes. Because the phagocytosis of photoreceptor disks by the RPE has been shown to be critical for photoreceptor cell viability, this defect likely contributes to the progressive blindness in USH1B.

Myosin VIIa is an unconventional myosin, now shown to possess the hallmarks of a myosin motor, namely, Mg^{2+} ATPase activity and the ability to move along actin filaments (1, 2). It is present in a variety of tissues (3, 4), but its most critical functions are in the inner ear and retina. Mutations in *MYO7A* cause Usher syndrome type 1B (USH1B; ref. 5), which accounts for 30–60% of USH1 (6). USH1 patients are born profoundly deaf, have vestibular dysfunction, and develop retinal degeneration, usually as teenagers (7).

Shaker1 mice possess mutant *Myo7a* (8, 9), and are deaf and have vestibular dysfunction. They do not undergo photoreceptor degeneration, unless also compromised by mutant *Cdh23* (10), another USH1 orthologue (11). However, they have abnormal electroretinograms (12), plus two other retinal mutant phenotypes, which have been identified by microscopy. One of these phenotypes is the absence of melanosomes from the apical processes of mutant retinal pigment epithelium (RPE; ref. 13). The simplest explanation of this observation is that myosin VIIa normally transports melanosomes (in an apical direction). The recent finding of a protein, MyRIP, that binds myosin VIIa and also Rab27a, a melanosome-binding G-protein, supports this suggestion (14). The other mutant phenotype is a slower rate of disk membrane renewal (15).

The renewal of disk membranes involves the continual addition of new disks at the base of the photoreceptor outer segment (16), and the periodic phagocytosis of the distal-most disks by the RPE (17). It was suggested that retarded disk membrane renewal in shaker1 retinas might be caused by the delivery of insufficient photoreceptor membrane to the site of disk membrane morphogenesis (15). Myosin VIIa is present at this site, in the connecting cilium (18), and an abnormally high accumulation of opsin was evident in the connecting cilia of shaker1 retinas (15). However, disk membrane renewal could be affected by perturbed RPE phagocytosis, and myosin VIIa is also present in the RPE; indeed well over 90% of retinal myosin VIIa seems to be located in the apical region of the RPE (3). Thus, it is fair to speculate that, in addition to a role in melanosome localization, myosin VIIa might be involved in the phagocytosis of disk membranes. This notion has been supported by studies on *Dictyostelium* myosin VII, which has been shown to have a role in phagocytosis. A null mutation for myosin VII results in inhibited ingestion by *Dictyostelium*, leading to the suggestion that myosin VII is responsible for the delivery of adhesion molecules to the cell surface (19, 20).

In the present study, we investigated the phagocytosis of disk membranes by *Myo7a* null RPE. We report that Myo7a is indeed required for normal phagocytosis of disk membranes. However, in contrast to myosin VII in *Dictyostelium*, our results indicate that Myo7a is important for events subsequent to initial ingestion.

CELL BIOLOGY

Materials and Methods

Animals. Shaker1 mice carrying the 4626SB allele were used. They possess a Gln720Stop mutation in *Myo7a* (9), which results in an effective null (15, 21). The mice were derived from those described (15). Two breeding colonies were used. One had been backcrossed to the BALB/c background, and then intercrossed. They were thus albino. These mice were used for the *in vivo* study, because the lack of pigment in the RPE facilitated phagosome identification. The other colony had been backcrossed to the CBA/CaJ background, and then intercrossed. These mice were pigmented and used for the RPE cell culture experiments, in which the presence of pigment in the RPE facilitated identification of the RPE cells during isolation. Mice were bred from homozygous × heterozygous parents, thus yielding homozygous mutant and heterozygous control littermates. The breeders and the resulting litters were all maintained on a 12-hr light/12-hr dark cycle, with exposure to 10–50 lux of fluorescent lighting during the light phase, and were treated according to National Institutes of Health and University of California at San Diego animal care guidelines. Homozygous mutants were distinguished from the heterozygous controls by their hyperactivity, head-tossing, and circling behavior, due to

This paper was submitted directly (Track II) to the PNAS office.

Abbreviations: RPE, retinal pigment epithelium; ROS, rod outer segment; GM, growth medium; DAPI, 4,6 diamidino-2-phenylindole dihydrochloride; USH1B, Usher syndrome type 1B.

*D.G. and J.K. contributed equally to this work.

†To whom correspondence should be addressed at: Department of Pharmacology, School of Medicine, University of California at San Diego, Mail Code 0912, 9500 Gilman Drive, La Jolla, CA 92093-0912. E-mail: dswilliams@ucsd.edu.

vestibular dysfunction (8). The genotypes of the young mice, used for RPE cell culture, were checked by a PCR/restriction digest assay, because the behavioral phenotype is less robust at this age.

Quantification of Phagosomes *in Vivo*. For 1 wk, animals were kept under the same light cycle, except that during the light phase, the light intensity was 50–200 lux of fluorescent lighting. They were then killed at specific times around the onset of the light. Their eyes were removed immediately and fixed in 2% paraformaldehyde + 2% glutaraldehyde in 0.1 M cacodylate buffer. Eyecups were processed for embedment in Epon. Semithin sections (0.7 μm) were obtained along the entire dorso-ventral axis, passing through the optic nerve head, and stained with 0.25% toluidine blue in 0.1% sodium borate. Phagosomes with diameters of at least 75% of the mean diameter of the rod outer segments (ROSs) in the given section ($\approx$0.9 μm) were counted along the entire section. Phagosomes in one complete section of one eye were counted for each animal. For phagosome counts, the following number of animals was used at the different times relative to lights-on (controls first, mutants second): 3 controls, 2 mutants ($-$120 min); 4, 4 ($-$60 min); 3, 4 ($-$30 min); 18, 16 (0 min); 11, 11 (30 min); 15, 15 (60 min); 11, 11 (90 min); 6, 7 (120 min); 2, 2 (150 min); 2, 1 (180 min); 2, 1 (360 min). The relative size (volume) of all control and mutant phagosomes included in these counts at lights-on and at 30 min after lights-on was calculated from their measured diameters in semithin sections, assuming a spherical shape and assuming that the extent of off-center sectioning was the same for mutant and control phagosomes. Phagosomes were also determined to be in the RPE apical region or the cell body, and the location of each phagosome with respect to its distance from the basal surface of the RPE was recorded. For phagosome location, the following number of animals was used: 3 controls, 2 mutants ($-$120 min); 4, 3 ($-$60 min); 3, 4 ($-$30 min); 14, 13 (0 min); 9, 9 (30 min); 8, 11 (60 min); 6, 6 (90 min).

All data on phagosomes were obtained by one of us (J.K.) under ''blind'' conditions, so that the genotype was not evident during the counting and measuring. These conditions were permitted by the use of albino mice; pigmented retinas are clearly identifiable as mutant or control by a previously described mutant phenotype, the mislocalization of RPE melanosomes (13). Our counts of phagosomes in control retinas were higher than those reported previously for mouse retinas (22, 23). It is noteworthy, however, that in these previous studies, counts were not made from retinas right at the time of peak shedding (30 min after light onset). Moreover, pigmented mice were used, so that only very new phagosomes could be discerned by light microscopy. There are no published data for albino mouse retinas, but our control phagosome numbers are similar to those reported from albino rat retinas (24).

Mouse Primary RPE Cell Isolation and Culture. We developed a procedure for mouse RPE culture based on the methods described for rat RPE cells (25, 26). Intact eyes were removed from 10- to 15-day-old mice. Lots of 10 eyes each were washed twice in 5 ml DMEM containing high glucose, then incubated with 5 ml 2% (wt/vol) Dispase, in DMEM for 45 min at 37°C. They were then washed twice in growth medium (GM) that consisted of DMEM (high glucose) plus 10% bovine FCS, 1% penicillin/streptomycin, 2.5 mM L-glutamine, and 1× MEM nonessential amino acids. All media and additives were from Invitrogen. An incision was made around the ora serrata of each eye, and the anterior cornea, lens, capsule, and associated iris pigmented epithelium were removed. The resulting posterior eyecups were then incubated in GM for 20 min at 37°C to facilitate separation of the neural retina from the RPE. After removal of the neural retina, intact sheets of RPE cells were peeled off the underlying basement membrane (Bruch's membrane) and transferred into a sterile 60-mm culture dish, containing 5 ml of fresh GM. The sheets of RPE were washed three times with GM and twice with Ca^{2+}- and Mg^{2+}-free Hanks' balanced salt solution (5 mM KCl/0.5 mM KH_2PO_4/4 mM $NaHCO_3$/150 mM NaCl/3 mM $Na_2HPO_4{\cdot}7H_2O$/5 mM glucose/0.05 mM phenol red, pH 7.4), and then briefly triturated by using a fine point Pasteur pipette. RPE cells were sedimented by centrifugation at 200 × *g* for 5 min and resuspended in GM to a final concentration of 50,000 cells per ml. Cells in suspension (0.5 ml) were added to the upper chamber of a 12-well plate, containing polycarbonate transwell inserts, with a 3.0-μm-pore diameter (Costar). GM (1 ml) was added to the lower well. Cells were cultured for 7 to 10 days until confluent colonies were present. Cultures showed no contamination with fibroblasts or choroidal cells based on microscopic analysis of cell morphology.

ROS Phagocytosis Assay. ROSs were isolated and purified from adult *Myo7a*^{4626SB} mouse retinas as described previously (27). Purified ROSs were resuspended in GM at a concentration of 5×10^7 ROSs per ml. ROSs were incubated with 7–10 day cultures of primary RPE cells by adding 0.5 ml of ROS suspension to the upper well of a 30-mm transwell plate. Note that this method rapidly exposes the RPE cells to ROSs, and thus differs from most published studies using other RPE cell cultures, where fewer ROSs were added in a larger volume. After the addition of ROSs, cells were incubated at 37°C, 5% CO_2 in a humidified incubator before fixation and immunocytochemical analysis. To assay ROS degradation, RPE cells were incubated with purified ROSs as above. After a 5-min incubation, unbound ROSs were removed by extensive washing with GM, and the cells were replaced in the incubator for either a 25-min or 55-min chase period before fixation and immunocytochemical analysis.

Double immunofluorescence labeling of bound and total ROSs was performed by using a bovine opsin polyclonal antibody, pAb01 (15), and the method described for rat RPE (28). Briefly, RPE cells that had been incubated with purified ROSs were washed vigorously three to four times in PBS (1.0 mM KH_2PO_4/155 mM NaCl/3 mM $Na_2HPO_4{\cdot}7H_2O$, pH 7.4) to remove any loosely associated ROSs. The cells were fixed with 4% paraformaldehyde in PBS, and the bound (but not ingested) ROSs were labeled with opsin antibody (pAb01), followed by an Alexa 488-nm conjugated goat anti-rabbit monoclonal antibody (Molecular Probes). Cells were then washed repeatedly in PBS buffer and made permeable with 47.5% ethanol for 15 min at room temperature. After removal of the ethanol and rehydration, both bound and ingested ROSs were labeled, by using the same opsin antibody, followed by an Alexa 594-nm conjugated goat anti-rabbit monoclonal antibody (Molecular Probes). Cells were washed in PBS, and nucleic acids were stained with 300 nM DAPI (4,6 diamidino-2-phenylindole dihydrochloride) in PBS. The transwell filters were excised and mounted under coverglass by using Vectashield (Vector Laboratories) anti-fade mounting medium. Ingested ROSs were determined by subtracting the bound ROSs from the total (bound plus ingested) ROSs. ROSs (at least 1 μm in diameter) were counted at ×750 magnification in all of the cells in a field of view (usually two to three) randomly selected from confluent areas of the filter. Typically $\approx$90% of the cells had ingested ROSs.

Microscopy and Image Analysis. Images of retinal sections and primary RPE cells were collected with a Zeiss Axiophot microscope, equipped with an ORCA C4742-95 charge coupled device (CCD) camera. Image acquisition and analysis was performed by using the OPENLAB V.2.2.5 software package. The 3D distribution of ingested ROSs in cultured primary RPE cells was examined by wide field microscopy (WFM), by using the 60 × 1.40 numerical aperture oil immersion objective on an inverted

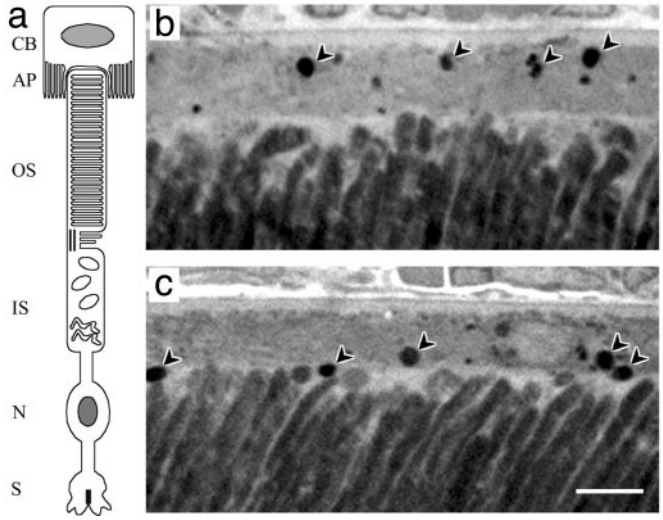

Fig. 1. Phagosomes in the RPE. (*a*) Diagram of photoreceptor and RPE cells. RPE cell: CB, cell body; AP, apical processes. Photoreceptor cell: OS, outer segment; IS, inner segment; N, nucleus, S, synapse. (*b* and *c*) Light micrographs of outer retina of control (*b*) and mutant (*c*) albino mice, fixed at 60 min after lights-on. Arrowheads indicate phagosomes that were counted. In *b*, the second arrowhead from the right indicates a phagosome that was just above the minimum size; immediately above this phagosome is another phagosome that was just below the minimum size, and so was not included in the count. Note that the phagosomes in the mutant RPE are located more apically than those in the control RPE. The apical RPE is stained less heavily than the rest of the cell (scale bar = 5 μm).

Olympus (Melville, NY) IX-70 DeltaVision Restoration microscope. The microscope was equipped with DAPI (360/40 excitation, 457/50 emission), FITC (490/20 excitation, 528/38 emission), and tetramethylrhodamine B isothiocyanate (TRITC; 555/28 excitation, 617/73 emission) band pass filter sets, a Bioptechs (Butler, PA) FCS2 motorized stage, and a Photometrics (Tucson, AZ) CH350 CCD camera. Optical sections were collected at 0.2-μm intervals along the apical-basal axis (65 sections per cell from the middle of the filter). Image stacks were then deconvolved, by using the DeltaVision constrained iterative deconvolution algorithm, and 3D projections were rendered by using the SOFTWORX V.2.5 analysis package, running on a Silicon Graphics (Mountain View, CA) Octane 250 R10/512. The number of ROSs per 0.2-μm optical section was quantified by using the NIH IMAGE J analysis package. A χ^2 test was used to determine the probability of no significant difference in the distribution of ingested ROSs between control and mutant RPE cells.

Results

Phagocytosis *in Vivo*. The phagocytosis of the distal disks from mammalian rod photoreceptor cells by the RPE is controlled by a circadian rhythm and peaks at dawn, or light onset (24, 29). We counted the number of phagosomes in the RPE of shaker1 mutant (*Myo7a*$^{4626SB/4626SB}$) and control (*Myo7a*$^{+/4626SB}$) retinas (Fig. 1), fixed at different times of day. In the mutants, there was still a peak in disk membrane phagocytosis, similar to that in control retinas. However, before the peak, just before lights-on, there were fewer phagosomes present in mutant RPE (Fig. 2*a*).

A further difference was evident when the subcellular localization of the phagosomes was determined. Before lights-on and for an hour after lights-on, there were proportionally more phagosomes in the apical processes of the mutant RPE (Fig. 2*b*). Although there were fewer phagosomes in the mutant RPE overall before lights-on, the apical processes of mutant and control RPE contained a similar number, due to this difference

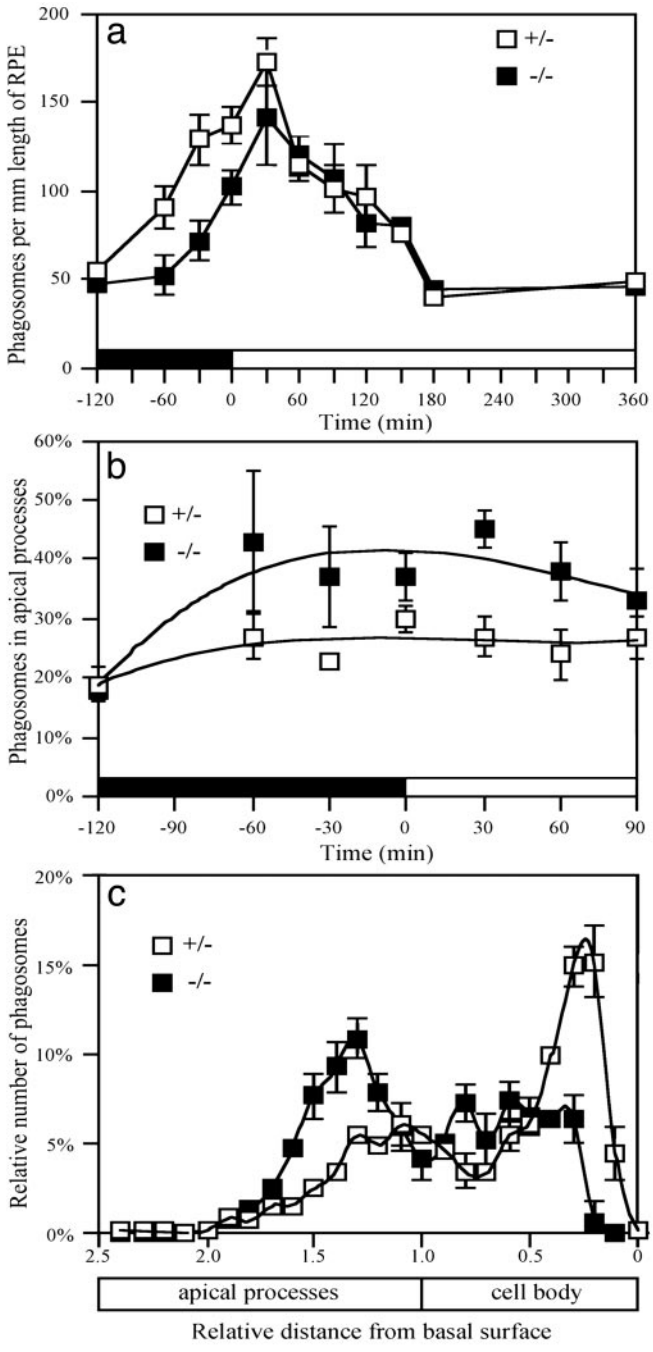

Fig. 2. Phagocytosis *in vivo*. (*a*) The total number of phagosomes in the RPE at different times of day. Phagosomes were counted in albino animals, so that they were observed clearly throughout the RPE cells by light microscopy. Previous studies on phagosomes in mouse RPE have used only pigmented animals, so that only very new phagosomes could be discerned (22, 23). Our total phagosome numbers in control retinas are thus greater than those reported in these studies, but they are comparable to those reported in albino rats (24). (*b*) The proportion of phagosomes just in the apical processes of the RPE is greater in mutants, during a 2-h period around the time of lights-on. (*c*) The location of the phagosomes within the RPE at 30 min after the time of light onset. In control retinas, phagosomes have aggregated in the basal region of the RPE, whereas, in mutant retinas, the largest aggregation is in the apical processes. The distance of the center of each phagosome from the basal surface was measured. Measurements for all phagosomes from a given retina were then normalized, with respect to a distance of 1.0 for the boundary between the cell body and apical processes. Error bars indicate ± SEM.

in relative distribution within the RPE. At 30 and 60 min after light onset, phagosomes were actually more abundant in the apical processes of the mutants compared with controls.

The processes of disk shedding and ingestion are inseparable in normal retinas, so that shed disks are not found in the extracellular space (30–32). We determined by electron microscopy (not shown) that all shed disks in the mutant retinas were contained within the RPE, indicating that the retinas are normal in this respect. However, freshly ingested phagosomes soon move from the apical region of the RPE into the cell body, and accumulate in the base of the cell, where they are degraded (17, 24, 33–35). This behavior is also clear from our localization data of phagosomes in control retinas. For example, at 30 min after light-onset (when the total number of phagosomes was the highest), phagosomes were most concentrated near the basal surface of the RPE (Fig. 2*c*). In mutant RPE, from 60 min before light-onset until 120 min after light-onset, those phagosomes that had been removed from the apical region were not concentrated near the basal surface (e.g., Fig. 2*c*). Hence, not only is the removal of phagosomes from the apical region into the cell body inhibited in mutant RPE, but transport all of the way to the basal region seems to be impeded.

Inhibited clearance of phagosomes from the apical processes should result in slower degradation, because phagosomes in the RPE do not fuse with lysosomes until they reach the cell body (33–35). Consistent with this expectation, the phagosomes counted at lights-on and at 30 min after lights-on were determined to be 13% and 14% larger, respectively, in mutants compared with controls ($P < 0.001$, in both cases), although this may be an underestimate given that phagosomes less than 0.9 μm were not counted in either the mutant or control retinas.

Phagocytosis by RPE Cells in Primary Culture. To dissect the process of RPE phagocytosis further, we studied RPE cells grown to confluency in primary culture. As described for rat RPE cells, these cells phagocytose ROSs, although not in a circadian-regulated manner. A concentration of 5×10^7 ROSs per ml seemed to be saturating for the ingestion of ROSs, consistent with a previous report that found that ingestion by primary cultures of human RPE cells was saturated with 1×10^7 bovine ROSs per ml (36). In our case, providing up to 10-fold more ROSs (5×10^8 per ml) resulted in no increase in ingestion. When 5×10^7 ROSs per ml were left as a continuous supply to the RPE cells, a similar number of ROSs were associated with mutant and control cells, irrespective of whether they were fed ROSs from control or mutant retinas. The number was the same after 5 min and after 60 min, and, in all cases, there was no significant difference in the percentage of ingested ROSs (≈80%; Fig. 3*a*). In this respect, phagocytosis *in vivo* and in culture differed.

The relative localization of the ingested ROSs within the cultured RPE cells was determined by using wide field deconvolution microscopy and quantitative analysis of optical sections taken at fixed intervals along the apical-basal axis of the cells (Fig. 3 *b* and *c*). ROSs were localized more apically in mutant RPE cells than in control cells, irrespective of whether the ROSs were from control or mutant retinas. This difference in localization was evident at both 5 min and 60 min after the addition of the ROSs (Fig. 3 *d* and *e*). After 60 min, the ingested ROSs in mutant RPE cells had aggregated in a more defined area; however, this area was still more apical than in the control cells (Fig. 3*e*).

When ROSs were added and then chased from the external medium after 5 min by extensive washing, a similar difference in localization of the ingested ROSs was observed between mutant and control RPE. In this experiment, we were able to determine the rate of degradation of the ingested ROSs by quantifying ROSs remaining after the 5-min "pulse." In mutant RPE cells, degradation was two times slower than in the controls (Fig. 3 *f* and *g*).

Discussion

Our results show that, in the absence of myosin VIIa, both *in vivo* and in cell culture, ingested phagosomes are not cleared normally from the RPE apical processes into the cell body. The studies on cultured RPE cells demonstrate that the fault is isolated in the RPE cells; it was evident even when the cells were fed control ROSs. The defect results in slower degradation of the phagosomes. In addition, it might account for the overall lower number of phagosomes in the mutant RPE *in vivo*.

If the ingestion of disk membranes is regulated to some extent by the presence of phagosomes still in the apical region, or by a stimulus provided on their removal, ingestion could be inhibited in the mutant because of phagosome retention in this region. Both before and after light onset, there were at least as many phagosomes in the RPE apical processes of the mutants as in those of the controls, despite fewer phagosomes throughout the cell at some of the times-of-day. Alternatively, reduced phagocytosis in the mutant could be a result of slower protein transport and disk membrane morphogenesis in the photoreceptor cells (15). The lack of a difference in the total number of phagosomes between mutant and control RPE cells in culture may be related to the fact that ingestion is not as well regulated in culture. It occurs whenever the RPE cells are presented with ROSs, not on a circadian rhythm (28), whole or partial ROSs are ingested (so phagosomes are of variable size), and there are many more phagosomes per cell than *in vivo*. The inhibition of ingestion *in vivo* was clear just before light onset. After light onset, a similar number of phagosomes were observed in mutant and control. However, given that the phagosomes seem to have a longer half-life in the mutant RPE, a lower ingestion rate likely persists after light onset as well.

There are two aspects of our findings that are potentially relevant to photoreceptor degeneration in USH1B. The first concerns the decreased ingestion rate observed *in vivo*. It is known from studies of rats, carrying a null mutation in the *Mertk* gene, that blockage of disk membrane ingestion leads to photoreceptor cell degeneration (37, 38). Although the absence of myosin VIIa does not result in blockage of disk membrane phagocytosis, its inhibition is likely to be relevant to a progressive blindness that first manifests itself after more than a decade, as in USH1B. The second consequence of lack of myosin VIIa is that phagosomes are degraded more slowly. Retarded degradation, in itself, could also be deleterious to the RPE and photoreceptor cell viability over a period. Inhibited lysosomal degradation is relevant to a variety of progressive disorders, including lysosomal storage diseases. In rats, treatment with lysosomal protease inhibitors seems to decrease RPE phagosome digestion with pathological consequences to the RPE and photoreceptor cells (39). Impaired phagosome degradation is thought to be responsible for the accumulation of drusen in age-related macular degeneration (40, 41), as well as lipofuscin accumulation in the RPE of the ABCR knockout mouse (42) and humans with Stargardt's disease (43), age-related macular degeneration (44), and some forms of retinitis pigmentosa (45). It is not known whether old shaker1 retinas have lipofuscin or drusen accumulations (mice need to be aged for this study). Nevertheless, the extended half-life of the phagosomes in the absence of myosin VIIa, even though there are fewer phagosomes formed, may be harmful.

Previously, it was proposed that the observed retardation of disk membrane renewal in the shaker1 retina was due to slower transport through the connecting cilium, as a greater accumulation of opsin was observed in this structure (15). As noted above, this photoreceptor defect might cause the decreased ingestion observed by the RPE *in vivo*. The addition of new disk

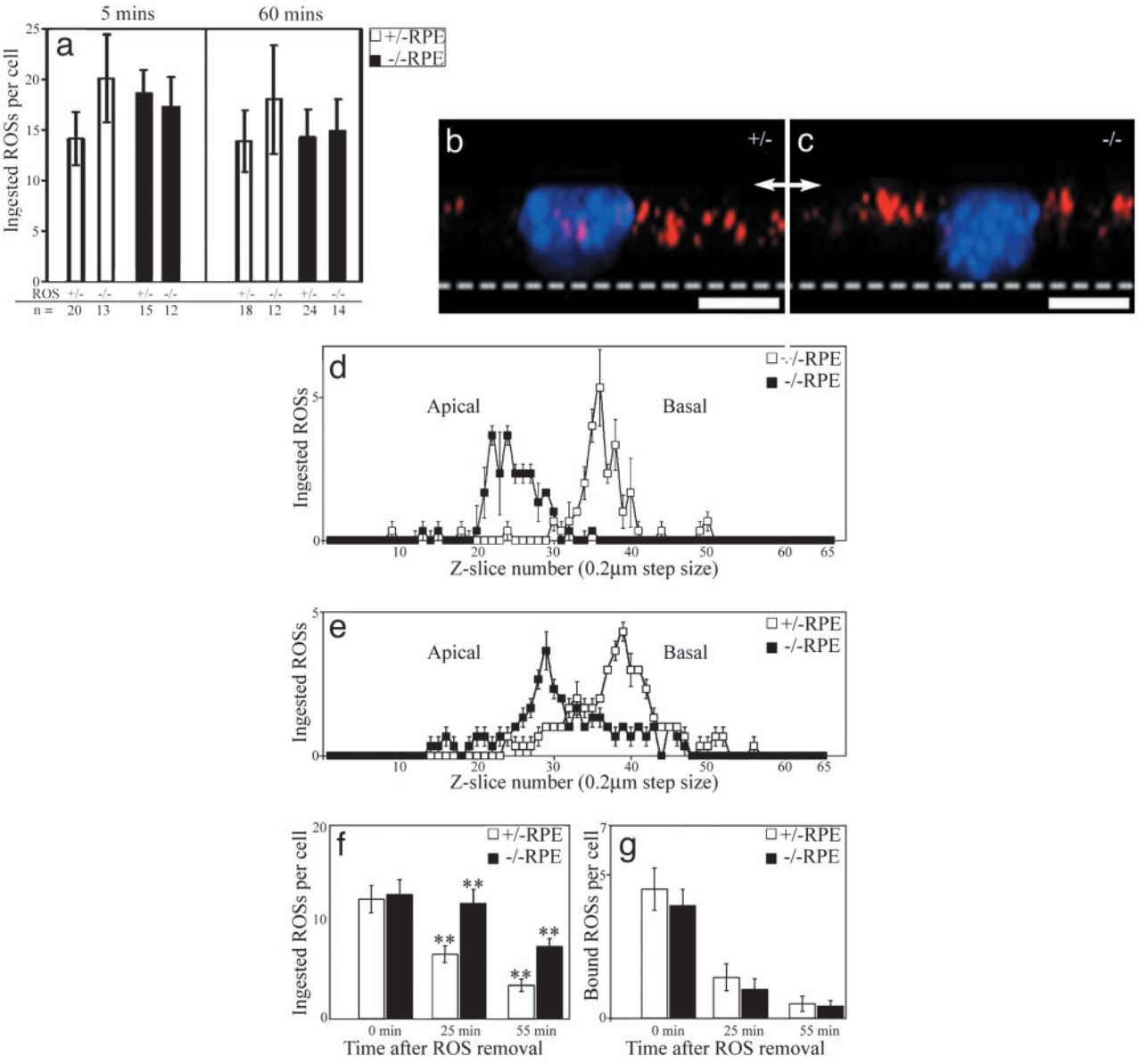

Fig. 3. Phagocytosis by RPE cells in primary culture. (*a*) Quantification of ingested ROSs. Mutant (−/−) and control (+/−) ROSs ingested by mutant and control RPE cells, 5 min and 60 min after excess ROSs were added. A similar number of ingested ROSs are found in all cases. Error bars indicate ± SD, *n* = number of cells, which were pooled from samples from four separate filters from two separate experiments. (*b* and *c*) Clearance of ingested ROSs in mutant RPE cells is inhibited. Wide-field epifluorescence image stacks were collected, deconvolved, and used to render 3D reconstructed images from control (*b*) or mutant (*c*) primary RPE cells after incubation with purified control ROSs for 5 min before fixation. Shown here are images of cells rotated through 90° so that the basal surface is at the bottom (dotted line) and the apical surface is uppermost (arrows). Ingested ROSs were labeled with anti-opsin/Alexa 594 nm and are colored red. Nuclei were labeled with DAPI and are colored blue. Ingested ROSs were localized more apically in the mutant RPE (scale bar = 10 μm). (*d* and *e*) The apical-basal distribution of ingested ROSs in control and mutant RPE was quantified after 5 min (*d*) or 60 min (*e*) incubation with purified ROSs (*n* = 3 cells in each case). The middle of the filter was in section 65, the RPE basal surface was about section 55, and the middle of the nucleus was about section 33. At both time points, the probability of no significant difference in ROS distribution between control and mutant RPE was <0.005 by χ^2 analysis. (*f* and *g*) Slowed ROS degradation in mutant RPE. The number of ingested (*f*) and bound (*g*) ROSs per cell were quantified after a 5-min pulse of ROSs, followed by a chase of either 25 min or 55 min after the ROSs were removed (*n* = 24 cells per treatment). No significant difference was observed in the number of ingested ROSs per cell after 5 min, or in the number of bound ROSs per cell at any time. However, at both the 30-min and the 60-min time points after the addition of ROSs, the number of ingested ROSs remaining in mutant RPE was double that in control RPE (**, $P < 0.001$). Error bars indicate ± SEM in *d–g*.

membrane at the base of the outer segment and phagocytosis of the distal disk membranes seem to be directly coupled in mouse (22). An alternative hypothesis is that the decreased phagocytosis we describe here could cause the retarded rate of disk membrane renewal. At present, there is no way to conclude which is the primary event. Determination of whether lack of myosin VIIa function in the photoreceptors, or the RPE, or both, is detrimental to vision is important for successful gene therapy of USH1B blindness. Although the present study does not rule out a critical function in the photoreceptor cells, it has isolated a potentially serious defect in the RPE (inhibited clearance of phagosomes) and thus indicates that the RPE should be included as a target for gene therapy. In this respect, it is noteworthy that gene therapy of the RPE seems promising (46, 47).

The last point for discussion concerns the cellular function of myosin VIIa in the RPE. The apical region of the RPE is rich in

actin filaments, so that the simplest explanation of the observed phenotype is that normal rapid clearance of phagosomes from the apical region involves transport by myosin VIIa along these filaments. However, most (70%) of the actin filaments in the apical RPE are oriented with their plus ends apically (B. Burnside, unpublished results in ref. 48). Myosin VIIa is a plus-end-directed motor (2). Apical transport of melanosomes by myosin VIIa (13) could therefore use the majority of the actin filaments, whereas basal transport of phagosomes would be limited to the minority. Myosin VIIa may have a less direct role in phagosome transport. Given the similarity between melanosomes and lysosomes, one suggestion is that myosin VIIa transports both types of organelle into the apical processes, and the fusion of lysosomes with the phagosomes is somehow important for their basal transport. However, phagosomes do not seem to fuse with lysosomes until they have been cleared from the apical processes (33–35). Moreover, by using cathepsin D and LAMP1 antibodies as markers for lysosomes, we found that the distribution of lysosomes in mutant RPE seemed normal (unpublished results), unlike that of the melanosomes. Furthermore, phagosome-lysosomal fusion depends on microtubules (49), and this dependence seems to result from transport of the phagosome to the lysosome (rather than the other way around) by microtubule motor(s). The basal movement of phagosomes in the RPE is blocked by the microtubule depolymerizing agent colchicine (33), suggesting the involvement of a plus-end-directed kinesin, given the orientation of the microtubules in the RPE (50). In macrophages, phagosomes are moved along microtubules by a kinesin and a dynein (51). In addition, myosin Va has been shown to be involved in this microtubule-dependent delivery of phagosomes to lysosomes in macrophages (52). Thus, an alternative suggestion is that myosin VIIa plays an auxiliary or regulatory role in microtubule motor transport of phagosomes from the apical RPE. Interestingly, such a role for myosin VIIa may be similar to that in the photoreceptor cilium, where myosin VIIa seems to participate in opsin transport (15), along with kinesin II, which seems to be the major motor for this function (53, 54).

We thank Dennis Defoe, Toshka Abrams, and Michael Hall for helpful discussions during our attempts to establish a procedure for the primary culture of mouse RPE cells, Dean Bok for cathepsin D antibodies, and Xianjie Yang for critical reading of the manuscript. This research was supported by National Institutes of Health Grant EY07042, National Institutes of Health Core Grant EY12598, and a grant from the Foundation Fighting Blindness.

1. Udovichenko, I. P., Gibbs, D. & Williams, D. S. (2002) *J. Cell Sci.* **115,** 445–450.
2. Inoue, A. & Ikebe, M. (2003) *J. Biol. Chem.* **278,** 5478–5487.
3. Hasson, T., Heintzelman, M. B., Santos-Sacchi, J., Corey, D. P. & Mooseker, M. S. (1995) *Proc. Natl. Acad. Sci. USA* **92,** 9815–9819.
4. Wolfrum, U., Liu, X. R., Schmitt, A., Udovichenko, I. P. & Williams, D. S. (1998) *Cell Motil. Cytoskeleton* **40,** 261–271.
5. Weil, D., Blanchard, S., Kaplan, J., Guilford, P., Gibson, F., Walsh, J., Mburu, P., Varela, A., Levilliers, J., Weston, M. D., *et al*. (1995) *Nature* **374,** 60–61.
6. Petit, C. (2001) *Annu. Rev. Genomics Hum. Genet.* **2,** 271–297.
7. Smith, R. J., Berlin, C. I., Hejtmancik, J. F., Keats, B. J., Kimberling, W. J., Lewis, R. A., Moller, C. G., Pelias, M. Z. & Tranebjaerg, L. (1994) *Am. J. Med. Genet.* **50,** 32–38.
8. Gibson, F., Walsh, J., Mburu, P., Varela, A., Brown, K. A., Antonio, M., Beisel, K. W., Steel, K. P. & Brown, S. D. M. (1995) *Nature* **374,** 62–64.
9. Mburu, P., Liu, X. Z., Walsh, J., Saw, D., Jamie, M., Cope, T. V., Gibson, F., Kendrick-Jones, J., Steel, K. P. & Brown, S. D. M. (1997) *Genes Funct.* **1,** 191–203.
10. Lillo, C., Kitamoto, J., Liu, X., Quint, E., Steel, K. P. & Williams, D. S. (2003) in *Retinal Degenerations: Mechanisms and Experimental Therapy*, eds. LaVail, M. M., Hollyfield, J. G. & Anderson, R. E. (Kluwer/Plenum, New York), in press.
11. Di Palma, F., Holme, R. H., Bryda, E. C., Belyantseva, I. A., Pellegrino, R., Kachar, B., Steel, K. P. & Noben-Trauth, K. (2001) *Nat. Genet.* **27,** 103–107.
12. Libby, R. T. & Steel, K. P. (2001) *Invest. Ophthalmol. Vis. Sci.* **42,** 770–778.
13. Liu, X., Ondek, B. & Williams, D. S. (1998) *Nat. Genet.* **19,** 117–118.
14. El-Amraoui, A., Schonn, J. S., Kussel-Andermann, P., Blanchard, S., Desnos, C., Henry, J. P., Wolfrum, U., Darchen, F. & Petit, C. (2002) *EMBO Rep.* **3,** 463–470.
15. Liu, X., Udovichenko, I. P., Brown, S. D. M., Steel, K. P. & Williams, D. S. (1999) *J. Neurosci.* **19,** 6267–6274.
16. Young, R. W. (1967) *J. Cell Biol.* **33,** 61–72.
17. Young, R. W. & Bok, D. (1969) *J. Cell Biol.* **42,** 392–403.
18. Liu, X., Vansant, G., Udovichenko, I. P., Wolfrum, U. & Williams, D. S. (1997) *Cell Motil. Cytoskeleton* **37,** 240–252.
19. Titus, M. A. (1999) *Curr. Biol.* **9,** 1297–1303.
20. Tuxworth, R. I., Weber, I., Wessels, D., Addicks, G. C., Soll, D. R., Gerisch, G. & Titus, M. A. (2001) *Curr. Biol.* **11,** 318–329.
21. Hasson, T., Walsh, J., Cable, J., Mooseker, M. S., Brown, S. D. M. & Steel, K. P. (1997) *Cell Motil. Cytoskeleton* **37,** 127–138.
22. Besharse, J. C. & Hollyfield, J. G. (1979) *Invest. Ophthalmol. Vis. Sci.* **18,** 1019–1024.
23. Grace, M. S., Chiba, A. & Menaker, M. (1999) *Vis. Neurosci.* **40,** 949–954.
24. LaVail, M. M. (1976) *Science* **194,** 1071–1074.
25. Mayerson, P. L., Hall, M. O., Clark, V. & Abrams, T. (1985) *Invest. Ophthalmol. Vis. Sci.* **26,** 1599–1609.
26. Chang, C. W., Roque, R. S., Defoe, D. M. & Caldwell, R. B. (1991) *Curr. Eye Res.* **10,** 1081–1086.
27. Tsang, S. H., Burns, M. E., Calvert, P. D., Gouras, P., Baylor, D. A., Goff, S. P. & Arshavsky, V. Y. (1998) *Science* **282,** 117–121.
28. Colley, N. J. & Hall, M. O. (1986) *Exp. Eye Res.* **42,** 323–329.
29. LaVail, M. M. (1980) *Invest. Ophthalmol. Vis. Sci.* **19,** 407–411.
30. Spitznas, M. & Hogan, M. J. (1970) *Arch. Ophthalmol.* **84,** 810–819.
31. Young, R. W. (1971) *J. Ultrastruct. Res.* **34,** 190–203.
32. Williams, D. S. & Fisher, S. K. (1987) *Invest. Ophthalmol. Vis. Sci.* **28,** 184–187.
33. Herman, K. G. & Steinberg, R. H. (1982) *Invest. Ophthalmol. Vis. Sci.* **23,** 277–290.
34. Herman, K. G. & Steinberg, R. H. (1982) *Invest. Ophthalmol. Vis. Sci.* **23,** 291–304.
35. Bosch, E., Horwitz, J. & Bok, D. (1993) *J. Histochem. Cytochem.* **41,** 253–263.
36. Kennedy, C. J., Rakoczy, P. E., Robertson, T. A., Papadimitriou, J. M. & Constable, I. J. (1994) *Exp. Cell Res.* **210,** 209–214.
37. Bok, D. & Hall, M. O. (1971) *J. Cell Biol.* **49,** 664–682.
38. Vollrath, D., Feng, W., Duncan, J. L., Yasumura, D., D'Cruz, P. M., Chappelow, A., Matthes, M. T., Kay, M. A. & LaVail, M. M. (2001) *Proc. Natl. Acad. Sci. USA* **98,** 12584–12589.
39. Okubo, A., Sameshima, M., Unoki, K., Uehara, F. & Bird, A. C. (2000) *Invest. Ophthalmol. Vis. Sci.* **41,** 4305–4312.
40. Eldred, G. E. (1998) in *The Retinal Pigment Epithelium*, eds. Marmor, M. F. & Wolfensberger, T. J. (Oxford Univ. Press, New York), pp. 651–668.
41. Crabb, J. W., Miyagi, M., Gu, X., Shadrach, K., West, K. A., Sakaguchi, H., Kamei, M., Hasan, A., Yan, L., Rayborn, M. E., *et al*. (2002) *Proc. Natl. Acad. Sci. USA* **99,** 14682–14687.
42. Weng, J., Mata, N. L., Azarian, S. M., Tzekov, R. T., Birch, D. G. & Travis, G. H. (1999) *Cell* **98,** 13–23.
43. Birnbach, C. D., Jarvelainen, M., Possin, D. E. & Milam, A. H. (1994) *Ophthalmology* **101,** 1211–1219.
44. Kliffen, M., van der Schaft, T. L., Mooy, C. M. & Jong, P. T. (1997) *Microsc. Res. Tech.* **36,** 106–122.
45. Kolb, H. & Gouras, P. (1974) *Invest. Ophthalmol. Vis. Sci.* **13,** 487–498.
46. Miyoshi, H., Takahashi, M., Gage, F. H. & Verma, I. M. (1997) *Proc. Natl. Acad. Sci. USA* **94,** 10319–10323.
47. Acland, G. M., Aguirre, G. D., Ray, J., Zhang, Q., Aleman, T. S., Cideciyan, A. V., Pearce-Kelling, S. E., Anand, V., Zeng, Y., Maguire, A. M., *et al*. (2001) *Nat. Genet.* **28,** 92–95.
48. King-Smith, C., Paz, P., Lee, C. W., Lam, W. & Burnside, B. (1997) *Cell Motil. Cytoskeleton* **38,** 229–249.
49. Malawista, S. E. (1975) *Ann. N.Y. Acad. Sci.* **253,** 738–749.
50. Troutt, L. L. & Burnside, B. (1988) *J. Cell Biol.* **107,** 1461–1464.
51. Blocker, A., Severin, F. F., Burkhardt, J. K., Bingham, J. B., Yu, H., Olivo, J. C., Schroer, T. A., Hyman, A. A. & Griffiths, G. (1997) *J. Cell Biol.* **137,** 113–129.
52. Al-Haddad, A., Shonn, M. A., Redlich, B., Blocker, A., Burkhardt, J. K., Yu, H., Hammer, J. A., Weiss, D. G., Steffen, W., Griffiths, G. & Kuznetsov, S. A. (2001) *Mol. Biol. Cell* **12,** 2742–2755.
53. Marszalek, J. R., Liu, X., Roberts, E. A., Chui, D., Marth, J. D., Williams, D. S. & Goldstein, L. S. (2000) *Cell* **102,** 175–187.
54. Pazour, G. J., Baker, S. A., Deane, J. A., Cole, D. G., Dickert, B. L., Rosenbaum, J. L., Witman, G. B. & Besharse, J. C. (2002) *J. Cell Biol.* **157,** 103–113.